In-situ pulsed laser induced growth of CdS nanoparticles on ZnO nanorods surfaces

In-situ pulsed laser induced growth of CdS nanoparticles on ZnO nanorods surfaces

Y. Rodríguez-Martínez[a], J. Alba-Cabañas[b], O. Cruzata[c], S. Bianco[d], E. Tresso[d], F. Rossi[e], L. Vaillant-Roca[a,*]

[a] Photovoltaic Research Laboratory, Institute of Materials Science and Technology – Physics Faculty, University of Havana, San Lázaro y L, 10 400, Havana, Cuba
[b] Physics Faculty, University of Havana, San Lázaro y L, 10 400, Havana, Cuba
[c] Laser Technology Laboratory, Institute of Materials Science and Technology, University of Havana, San Lázaro y L, 10 400, Havana, Cuba
[d] Department of Applied Science and Technology – DISAT, Politecnico di Torino, Corso Duca degli Abruzzi 24, 10129, Torino, Italy
[e] IMEM-CNR Institute, Parco Area delle Scienze 37/A, 43124, Parma, Italy

ABSTRACT

Herein we present a process for the in-situ growth of CdS nanoparticles using a pulsed laser irradiation. A Nd-YAG laser was applied to ZnO nanorods previously submerged in an aqueous precursor solution containing cadmium chloride and thiourea. For optimum values of the laser fluence, around 40 mJ/cm2 it was possible to fabricate a highly homogeneous film of CdS nanoparticles covering the ZnO nanorods surface. Cathodoluminescence measurements of the ZnO/CdS structure show the quenching of the ZnO yellow and green luminescence, indicating the ZnO surface defects passivation by CdS nanostructures. Although lasers have been already used for inducing growth in solution, this work presents new evidence of in-situ growth on the surface of nanostructured materials. The laser based technique presented is simple, easy to implement, scalable and it could be applied in the fabrication of nanostructured solar cells and other devices.

1. Introduction

Nanostructured architectures for solar cells have increasingly attracted the attention over the last two decades [1-3]. The extended use of nanostructures in solar cells represented a breaking point in the junction design by increasing the active area of interaction and the opportunities of selecting materials and growing techniques. The main driving force has been the promise of high efficiency - low cost solar cells using inexpensive technological processes and accessible and environmentally friendly materials [4,5]. At the same time, the great potential of exploiting the harvest of hot carriers as well as the multiple carrier generation in the case of quantum confinement have lead researchers to the search for new strategies to achieve these goals [6,7]. In general terms a mesoporous wide-band gap semiconductor can work as a scaffold for a multiple choice of sensitizers. TiO_2 and ZnO have been the most studied options as wide-bandgap materials forming nanoparticles or vertically aligned nanorods/nanotubes as well. For the absorber material several choices have been made like dyes (DSSC), conjugates polymers and inorganic semiconductors as films or quantum dots (extremely thin absorbers (ETA) solar cells and quantum dots solar cells (QDSC) respectively) [8-11]. The sensitizer plays the role of absorbing light and generating the photocarriers, giving by band gap engineering alignment an electron to the n-type oxide semiconductor scaffold. The positive charge should be conducted by a different path, using hole transport layers, electrolytes or directly into the rear electrode of the device. However, beyond the potential of nanostructured devices, there are still many challenges to overcome for achieving a stable, acceptably efficient and low-cost device. Among them, key roles are played by the selection of materials, the band engineering, the stability and the control of nanostructures sizes and morphologies by low cost techniques. Also, and perhaps the most important one, the interfacial electron and hole transfer must be optimized as the primary step for collecting the photogenerated carriers. Many of these issues can be connected to the nanostructures synthesis techniques and more specifically, to the method used for building the main interface. In the particular case of inorganic heterostructures, the growth of the heterostructure takes place generally by two methods, in-situ and ex-situ [12,13]. The ex-situ methods consist in the external fabrication of the sensitizer that should be latter coupled on the scaffold surface. Although the ex-situ method can provide a better nanostructure size and shape control, it presents a poorer surface coverage and limitations regarding the charge transfer process [13,14]. On the other hand, in the in-situ method the sensitizer is directly grown over the electron transport layer surface, giving rise to a direct connection which can even be epitaxially obtained [13]. These characteristics lead to a much better charge transfer between the sensitizer and the wide band gap material. Chemical Bath Deposition (CBD) and Successive Ionic Layer Adsorption and Reaction (SILAR) are the classical in-situ methods giving the possibility to improve the surface coverage by successfully infiltrating the scaffold [15,16]. Both cases imply the preparation of certain solution volumes as well as using time scales in the order of hours. In this work we are proposing a method for the fast growth (seconds) of inorganic heterostructures by means of an in-situ pulsed laser induced process. The laser as a source of energy for nanostructures growth has been used recently in different works [17-19]. Interesting cases are the patterned in-situ CdS nanocrystals into a polymer matrix [20] and the laser decomposition of zinc acetate for the digital selective growth of ZnO nanorods [21,22]. In our case we produce homogeneous nanoparticles on the scaffold surface for a particular range of laser fluences. The main advantage is the direct attachment of the light harvest material to the electron transport material. This allows a direct crystalline lattice connection between both materials that improves the efficiency of the charge transfer process. Moreover, the process requires minimum quantities of precursors solutions and can be totally performed in the scale of seconds. Another important advantage is its effectiveness on inter penetrating the scaffold providing a high surface coverage. Several inorganic sensitizers have been studied but the chalcogenides have probably been the most visited ones. Combination of CdS nanoparticles decorating ZnO nanorods, CdSe QDs sensitizing TiO_2 nanotubes, and CdS/CdSe core/shell QDs covering either ZnO or TiO_2 nanostructures, are some examples [23-25]. We have selected CdS, as a well-known material, to test the proposed laser-based method for sensitizing the ZnO nanorods surface.

2. Experimental

2.1. Materials and methods

2.1.1. ZnO seeds layer

Soda-lime glass and indium-tin oxide (ITO) coated glass were used as substrates to grow the core/shell structures. All the substrates were properly cleaned and washed before the seeding process, which is an important step to obtain vertically aligned nanorods as well as to guarantee the whole coverage of the substrate surface [26]. The ZnO seeds layer was grown by the spin-coating method as reported in previous works [22,27]. However, some sets of samples were intentionally obtained without the seeding process. In these cases, the ZnO nanorods are poorly vertically aligned and tend to create nanoflowers. This allows us a better exploring of the coverage along the nanorods surfaces.

2.1.2. ZnO nanorods

To grow poorly aligned nanorods, the no seeded substrates were suspended in a stirred solution of 50mM of zinc nitrate hexahydrate and hexamethylenetetramine (1:1M ratio) contained in a close system and heated at 90 °C for 1.5 h. On the other hand, to obtain vertically aligned nanorods, seeded substrates were placed horizontally, seeds upwards, in a no stirred solution to further simplify the previous approach. The samples were then washed with deionized water and dried with a nitrogen stream.

2.1.3. ZnO/CdS nanostructures

To fabricate the CdS shell structure, a 0.2M of cadmium chloride 2.5 hydrate and thiourea aqueous solution (1:1M ratio) was prepared. A volume of 80 μl of solution was dropped over the ZnO nanorods (Fig. 1a), covering the entire substrate surface. Then, a Nd: YAG laser (Bralax, 532 nm) was placed in such a way that the beam impacted perpendicularly the sample surface (Fig. 1b). We used fluences ranging from 10 mJ/cm$_2$ to hundreds of mJ/cm$_2$, but preventing the substrate damage. To establish the fluence value (±0.3 mJ/cm$_2$), the energy of the laser was fixed at 28 mJ and the distance laser-sample was changed. The samples were then irradiated at 13.2, 25.6, 42.3 and 61.7 mJ/cm$_2$. The number of laser-sample interactions, or shots, was also studied (2 and 5 shots), being 4 Hz the shots frequency in all the cases. The duration of the shot is of 100 μs. References laser-induced grown CdS samples were made on top of silicon substrates in order to differentiate the new laser grown species from those grown over the nanorods surfaces. A final experiment was also done in which the process of interaction is repeated in cycles trying to obtain a greater amount of deposited material on the nanorods surface. In this case the fluence and number of shots were fixed at 40.1 mJ/cm$_2$ and 2 respectively. The procedure was repeated from 1 to 5 times and after each cycle the samples were washed with deionized water and dried to eliminate unwanted residues originated from the solution.

2.2. Characterization

Morphological study and Energy Dispersive X-ray Spectrometry (EDS) measurements were performed using a ZEISS Merlin field emission SEM, while a PANalitycal X' Pert Pro diffractometer in Bragg/ Brentano configuration (Cu Kα X-ray source) was employed to study the crystalline structure of the samples. Raman spectra were measured by means of a Renishaw' s inVia micro-Raman spectrometer, equipped with a cooled CCD camera, with a laser excitation wavelength of 514.5 nm. For the Cathodoluminescence (CL) measurements a Gatan MonoCL, belonging to a S-360 Cambridge SEM, was used.

3. Results and discussion

The typical hexagonal ZnO nanorods morphology without previous seeding, as well as the morphologic characteristics of the laser induced heterostructures for different fluence values and 5 shots can be seen in the SEM images reported in Fig. 2. The micrographs show a progressive formation of condensed material coating the nanorods surface as the fluence increases. In particular, 42.3 mJ/cm$_2$ was the more effective fluence value, showing a complete coating of the nanorods. On the other hand, horizontal rods with a rounded appearance predominate when the fluence reaches 61.7 mJ/cm$_2$ (Fig. 2d). The reference samples of CdS grown on silicon substrates confirm that these elongated species are properly due to the interaction of the pulsed laser irradiation with the precursor CdS solution, as can be noticed in Fig. 2(f-h). A high surface coverage of the ZnO with a thin shell of CdS nanoparticles was obtained using a fluence of 41.7 mJ/cm$_2$ (close to the previous 42.3 mJ/cm$_2$ in Fig. 2c) but decreasing to 2 the number of shots. This complete decoration with CdS nanoparticles grown in-situ over the ZnO surface can be observed in Fig. 3 from a) to d). Images 3 e) and f) represent the EDS spectra for the sample before and after the laser induced process. In both cases it can be observed the peaks corresponding to Zn and O, as well as other peaks related with the substrate, principally Si. As can be noticed, after the laser interaction the spectrum contains additionally the Cd, Cl and S peaks. The intensity of Cd and Cl is higher compared with the S one, indicating the possible presence of precursor residues used in the aqueous solution, in particular $CdCl_2$. The low intensity of S can be explained by the presence of very thin layers of CdS deposited in the nanorods surface. For samples where the ZnO nanorods were grown after seeds deposition and using the no-stirring configuration in the chemical bath process (described in the experimental section), a higher nanorods density as well as a reduction of their diameters to around 50 nm was achieved (Fig. S1 of supplementary information). This is favourable for

Fig. 1. Laser induced growth to obtain the ZnO/CdS core/shell structures. Red circles in the experimental setup frame the laser (bigger circle) and the sample holder (smaller circle). The fluence and number of laser shots are the main studied parameters (For interpretation of the references to colour in this figure legend, the reader is referred to the web version of this article).

photovoltaic applications, where the optimal diameter is between 20 nm and 40 nm [28]. In this case, the laser induced process was done at 40.1 mJ/cm$_2$, 2 shots and repeated in 5 cycles. After each cycle the samples were washed and dried. We have obtained a homogeneous and granular covering of the nanorods surface, forming the desired ZnO/CdS core/shell structures without residues or features like nanoparticles, sheets or rods. We believe this is a result of the samples washing after each cycle. The laser-based technique resulted to be an in-situ method useful to infiltrate nanoparticles onto the ZnO nanorods scaffold surface. The characteristics of the final heterostructures to obtain depend on the values of the involved parameters (fluence and shots). Fig. 4 shows the X-ray diffraction (XRD) patterns for ZnO/CdS heterostructures corresponding to samples irradiated with 61.7 mJ/cm$_2$ (5 shots) and 41.7 mJ/cm$_2$ (2 shots), respectively. The presence of ZnO with hexagonal phase is revealed in both cases (JCPDS PDF # 03-0888), as well as some peaks corresponding to $CdCl_2$ (JCPDS PDF # 85-1266) precursor residues. Also, sample irradiated with 41.7 mJ/cm$_2$ shows the peaks corresponding to ITO substrate (JCPDS PDF # 89-4599). CdS peak can be observed for 61.7 mJ/cm$_2$, suggesting the growth of this material with hexagonal phase (JCPDS PDF # 75-1545) after the laser interaction. However, the sample irradiated with 41.7 mJ/cm$_2$ does not show any peak corresponding to CdS. These results can be due, in agreement with SEM images, to the presence of a very thin layer of material covering the nanorods for 41.7 mJ/cm$_2$ and the existence of condensed structures of CdS for 61.7 mJ/cm$_2$. Fig. 5 shows the Raman spectra of three samples: ZnO nanorods, ZnO/CdS (42.3 mJ/cm$_2$, 5 shots) and ZnO/CdS (61.7 mJ/cm$_2$, 5 shots). In each case, a comparison with standard patterns [29] corresponding to ZnO and CdS, both with hexagonal phase, has been made to determine the present phases in the samples. The graphs on the left show an evident correspondence between peaks from the ZnO nanorods sample and the ZnO standard, which means the nanorods have the same hexagonal phase. These peaks are also present in the laser irradiated samples as it was expected. The characteristic peaks of CdS, located between 150 cm^{-1} and 325 cm^{-1}, are present also for the two laser irradiated samples. On the other hand, peaks at 357 cm^{-1} and 474 cm^{-1} (marked with circles) are attributed to defects or residues from the fabrication process. This result, in addition to the XRD measurements, is a proof that CdS crystalline material grew using the laser technique. The CL spectrum corresponding to ZnO nanorods grown by CBD is shown in Fig. 6a. The pattern is mainly composed by two principal peaks centered at 3.21 eV and 2.18 eV, the former usually associated to the ZnO bandgap and the latter to defects present in the material. A Gaussian deconvolution allowed us to discern a minimum of emissions that could contribute to the broad peak at 2.18 eV and features like "shoulders" in the measured pattern. Then it was possible to find two peaks commonly attributed to the Yellow Luminescence (YL) and Green Luminescence (GL) at 2.17 eV and 2.51 eV respectively, as previously reported in literature [30,31]. YL is usually present in ZnO nanostructures grown by aqueous methods, that include zinc nitrate and HMT as precursors, and it is originated by oxygen interstitials not located at the surface [30]. On the other hand, GL is commonly related with oxygen vacancies, although there is a great controversy about what can cause it. Nevertheless, there are evidences suggesting the presence of the GL defects at the surface [31]. The peak located at 3.22 eV

Fig. 2. SEM images from the heterostructures obtained on glass by pulsed laser irradiation: a) ZnO/CdS (13.2 mJ/cm$_2$, 5 shots), b) ZnO/CdS (25.6 mJ/cm$_2$, 5 shots), c) ZnO/CdS (42.3 mJ/cm$_2$, 5 shots), d) ZnO/CdS (61.7 mJ/cm$_2$, 5 shots) and e) as grown ZnO nanorods (no seeded, stirred growth). Images f), g) and h) show the formation of rods-like structures after laser irradiation for three samples: Si/CdS (42.3 mJ/cm$_2$, 5 shots), ZnO/CdS (42.3 mJ/cm$_2$, 5 shots) and ZnO/CdS (61.7 mJ/cm$_2$, 5 shots), respectively. Black circles enclose those structures and dashed line in h) divides the zone where the laser impacted (left part) from the external zone.

Fig. 3. SEM images of: a) and c) ITO/ZnO nanorods before laser interaction (stirred growth), b) and d) ITO/ZnO/CdS sample where it was obtained the expected core/shell structure (41.7 mJ/cm2, 2 shots), e) and f) corresponding EDS spectra.

Fig. 4. XRD patterns for ZnO/CdS heterostructures irradiated with laser fluences of 41.7 mJ/cm2 (2 shots) and 61.7 mJ/cm2 (5 shots) respectively. SEM images have been added in each case to better understanding and visualization of the results.

corresponds to near-band-edge (NBE) transitions intrinsic of the ZnO nanorods [32], while the peak around 3.12 eV is attributed to transitions between the valence band and oxygen vacancies levels located at 0.05 eV below the conduction band [30]. In the case of the ZnO/CdS core/shell structures (41.7 mJ/cm2), the CL spectrum shows a unique broad peak centered at about 2.81 eV (Fig. 6b)). Both the YL and the GL emission decrease in the spectrum, suggesting that with the growth of the CdS layer on the nanorods surface, a big part of the ZnO superficial defects were passivated. As in the previous graph, a Gaussian fitting was made to obtain a better interpretation of the origin of the peak, which covers a wide spectral range. Then, a peak at 3.2 eV corresponding to the ZnO bandgap or excitonic transitions, and a weak peak around 2.4 eV were found, that can correspond with a remnant GL or the CdS NBE. In case of being attributed to CdS NBE, the low intensity of this peak may indicate that a part of the excited electrons is transferred to ZnO nanorods instead of recombining, due to the favorable coupling of the bands of the two materials, although it may also mean that the CdS layer is very thin. On the other hand, the peaks located at 2.73 eV and 2.98 eV have been observed when Cd impurities are introduced in the ZnO structure [33]. Also, these have been eventually attributed to blue emissions, in some cases due to oxygen or zinc vacancies in ZnO [30]. In general, zinc vacancies in this material are difficult to achieve [30], but a laser interaction has been able to produce them, as reported previously [34]. The EDS measurements (Fig. 3) show an increase of the O/Zn ratio after the laser irradiation. Therefore, we could relate the present blue emissions to zinc vacancies originated after the interaction sample laser. Another hypothesis is the presence of quantum confinement due to the appearance of small CdS nanocrystals, in case their sizes were in the order of the Bohr radius of the material. The result of this quantum

Fig. 5. Raman spectra corresponding to: (left) ZnO nanorods and ZnO standard pattern [29], (right) ZnO/CdS structures (42.3 mJ/cm2 and 61.7 mJ/cm2, 5 shots) and CdS standard pattern [29]. Peaks marked with circles are attributed to defects or residues.

Fig. 6. CL spectra is shown for ZnO nanorods before (a) and after (b) being covered with CdS by laser induced growth (41.7 mJ/cm2, 2 shots). The Gaussian deconvolution helps to understand the contribution of several effects to the original pattern.

effect is the shift of the fundamental transition to energies higher than the bandgap value of the bulk (2.4 eV). The high intensity of these peaks could be explained taking into account the noticeable increase of the superficial area of the material forming nanoparticles. That promotes electrons to recombine easily and do not be transferred to ZnO, due to a higher presence of defects at the surface. Considering this last hypothesis as possible, the obtained shell will be formed by CdS as bulk material and very small nanoparticles, which present quantum confinement. However, this hypothesis requires some additional analysis and measurements to be verified.

4. Conclusions

We present a laser-based technique as a useful in-situ tool to sensitize and infiltrate scaffold structures, like ZnO nanorods, with other functional material like CdS. The morphology of the as grown material and the extent of surface coverage of the nanorods, depends on the fluence and number of shots during laser treatment. The fluence of the laser influenced the formation of condensed shells on the ZnO nanorods surface or independent structures like CdS nanorods as well. Moreover, changing the number of shots, the method allowed to obtain thin shells formed of nanoparticles. In addition, experiments where the number of laser interaction cycles increased, showed more homogeneity in the growth. This laser based technique allows to growth the absorber materials directly onto the electron transport material surface, providing a better connection for the charge transfer process. It was corroborated the presence of hexagonal CdS and ZnO by means XRD and Raman spectroscopy. On the other hand, CL measurements before and after the laser irradiation indicated the passivation of surface defects of the nanorods with the CdS deposition, as the decreasing of green and yellow luminescence emissions suggested. Some hypothesis related to blue emission peaks in the laser irradiated sample, include doping of ZnO nanorods, creation of vacancies due to laser interaction and possible formation of nanocrystals with quantum behavior.

Acknowledgements

L. Vaillant-Roca acknowledges Politecnico di Torino, Italy, for the Visiting Professor position and Dr. E. Reguera for his support in the experimental work. This work is under the projects No. 17/2-2019 and No. 17/3-2019 of the National Program of Nanoscience and Nanotechnology (PN3), Cuba. This research did not receive any specific grant from funding agencies in the public, commercial, or not-for-profit sectors

References

[1] Matthew C. Beard, Joseph M. Luther, Arthur J. Nozik, The promise and challenge of nanostructured solar cells, Nat. Nanotechnol. 9 (2014) 951, https://doi.org/10.1038/nnano.2014.292.
[2] C.C. Raj, R. Prasanth, A critical review of recent developments in nanomaterials for photoelectrodes in dye sensitized solar cells, J. Power Sources 317 (2016) 120‑132, https://doi.org/10.1016/j.jpowsour.2016.03.016.
[3] Rui Yu, Qingfeng Lin, Siu-Fung Leung, Zhiyong Fan, Nanomaterials and nanostructures for efficient light absorption and photovoltaics, Nano Energy 1 (2012) 57‑72, https://doi.org/10.1016/j.nanoen.2011.10.002.
[4] Laurence M. Peter, Towards sustainable photovoltaics: the search for new materials, Philosophical Transactions of the Royal Society A: mathematical, Physical and Engineering Sciences 369 (2011) 1840‑1856, https://doi.org/10.1098/rsta.2010.0348.
[5] Ting Guo, Ming-Shui Yao, Yuan-Hua Lin, Ce-Wen Nan, A comprehensive review on synthesis methods for transition-metal oxide nanostructures, CrystEngComm 17 (2015) 3551‑3585, https://doi.org/10.1039/c5ce00034c.
[6] Mee Rahn Kim, Dongling Ma, Quantum-dot-Based solar cells: recent advances, strategies, and challenges, J. Phys. Chem. Lett. 6 (2015) 85‑99, https://doi.org/10.1021/jz502227h.

[7] Frederik Hetsch, Xueqing Xu, Hongkang Wang, Stephen V. Kershaw, Andrey L. Rogach, Semiconductor nanocrystal quantum dots as solar cell components and photosensitizers: material, charge transfer, and separation aspects of some device topologies, J. Phys. Chem. Lett. 2 (2011) 1879‑1887, https://doi.org/10.1021/jz200802j.
[8] Vipinraj Sugathan, Elsa John, K. Sudhakar, Recent improvements in dye sensitized solar cells: a review, Renewable Sustainable Energy Rev. 52 (2015) 54‑64, https://doi.org/10.1016/j.rser.2015.07.076.
[9] Gilles Dennler, Markus C. Scharber, Christoph J. Brabec, Polymer-fullerene bulkheterojunction solar cells, Adv. Mater. 21 (2009) 1323‑1338, https://doi.org/10.1002/adma.200801283.
[10] Thomas Dittrich, Abdelhak Belaidi, Ahmed Ennaoui, Concepts of inorganic solidstate nanostructured solar cells, Sol. Energy Mater. Sol. Cells 95 (2011) 1527‑1536, https://doi.org/10.1016/j.solmat.2010.12.034.
[11] Sandeep Kumar, Monika Nehra, Akash Deep, Deepak Kedia, Neeraj Dilbaghi, Ki-Hyun Kim, Quantum-sized nanomaterials for solar cell applications, Renewable Sustainable Energy Rev. 73 (2017) 821‑839, https://doi.org/10.1016/j.rser.2017.01.172.
[12] Sven Rühle, Menny Shalom, Arie Zaban, Quantum - dot - sensitized solar cells, ChemPhysChem 11 (2010) 2290‑2304, https://doi.org/10.1002/cphc.201000069.
[13] Rachel S. Selinsky, Qi Ding, Matthew S. Faber, John C. Wright, Song Jin, Quantum dot nanoscale heterostructures for solar energy conversion, Chem. Soc. Rev. 42 (2013) 2963‑2985, https://doi.org/10.1039/c2cs35374a.
[14] Gi-Hwan Kim, F. Pelayo García de Arquer, Yung Jin Yoon, Xinzheng Lan, Mengxia Liu, Oleksandr Voznyy, et al., High-efficiency colloidal quantum dot photovoltaics via robust self-assembled monolayers, Nano Lett. 15 (2015) 7691‑7696, https://doi.org/10.1021/acs.nanolett.5b03677.
[15] Ling Chen, Haibo Gong, Xiaopeng Zheng, Min Zhu, Jun Zhang, Shikuan Yang, Bingqiang Cao, CdS and CdS/CdSe sensitized ZnO nanorod array solar cells prepared by a solution ions exchange process, Mater. Res. Bull. 48 (2013) 4261‑4266, https://doi.org/10.1016/j.materresbull.2013.06.069.
[16] Youngjo Tak, Suk Joon Hong, Jae Sung Lee, Kijung Yong, Fabrication of ZnO/CdS core/shell nanowire arrays for efficient solar energy conversion, J. Mater. Chem. 19 (2009) 5945‑5951, https://doi.org/10.1039/b904993b.
[17] Vahid Najafi, Mehrnoush Aghelifar, Salimeh Kimiagar, A novel synthesis of CZTS quantum dots using pulsed laser irradiation, Superlattices Microstruct. 109 (2017) 702‑707, https://doi.org/10.1016/j.spmi.2017.05.063.
[18] L.V. Garcia, S.L. Loredo, S. Shaji, J.A. Aguilar Martinez, D.A. Avellaneda, T.K. Das Roy, B. Krishnan, Structure and properties of CdS thin films prepared by pulsed laser assisted chemical bath deposition, Mater. Res. Bull. 83 (2016) 459‑467, https://doi.org/10.1016/j.materresbull.2016.06.027.
[19] H. El Hamzaoui, R. Bernard, A. Chahadih, F. Chassagneux, L. Bois, B. Capoen, M. Bouazaoui, Continuous laser irradiation under ambient conditions: a simple way for the space-selective growth of gold nanoparticles inside a silica monolith, Mater. Res. Bull. 46 (2011) 1530‑1533, https://doi.org/10.1016/j.materresbull.2011.05.010.
[20] D. Fragouli, V. Resta, P.P. Pompa, A.M. Laera, G. Caputo, L. Tapfer, R. Cingolani, A. Athanassiou, Patterned structures of in situ size controlled CdS nanocrystals in a polymer matrix under UV irradiation, Nanotechnology 20 (2009) 155302, , https://doi.org/10.1088/0957-4484/20/15/155302.
[21] Sukjoon Hong, Junyeob Yeo, Wanit Manorotkul, Hyun Wook Kang, Jinhwan Lee, Seungyong Han, et al., Digital selective growth of a ZnO nanowire array by large scale laser decomposition of zinc acetate, Nanoscale 5 (2013) 3698‑3703, https://doi.org/10.1039/c3nr34346d.
[22] Y. Rodríguez-Martínez, J.A. Alba-Cabañas, O. Cruzata-Montero, L. Vaillant-Roca, Laser activation to growth ZnO nanostructures, Rev. Cubana Fis. 35 (2018) E21‑E23.
[23] H.K. Jun, M.A. Careem, A.K. Arof, Quantum dot-sensitized solar cells‒perspective and recent developments: a review of Cd chalcogenide quantum dots as sensitizers, Renewable Sustainable Energy Rev. 22 (2013) 148‑167, https://doi.org/10.1016/j.rser.2013.01.030.
[24] Heejin Kim, Hyuncheol Jeong, Tae Kyu An, Chan Eon Park, Kijung Yong, Hybridtype quantum-dot cosensitized ZnO nanowire solar cell with enhanced visible-light harvesting, ACS Appl. Mater. Interfaces 5 (2012) 268‑275, https://doi.org/10.1021/am301960h.
[25] Youngjo Tak, Suk Joon Hong, Jae Sung Lee, Kijung Yong, Fabrication of ZnO/CdS core/shell nanowire arrays for efficient solar energy conversion, J. Mater. Chem. 19 (2009) 5945‑5951, https://doi.org/10.1039/B904993B.
[26] Innocent Udom, Manoj K. Ram, Elias K. Stefanakos, Aloysius F. Hepp, D. Yogi Goswami, One dimensional-ZnO nanostructures: synthesis, properties and environmental applications, Mater. Sci. Semicond. Process. 16 (2013) 2070‑2083, https://doi.org/10.1016/j.mssp.2013.06.017.
[27] Lori E. Greene, Matt Law, Dawud H. Tan, Max Montano, Josh Goldberger, Gabor Somorjai, Peidong Yang, General route to vertical ZnO nanowire arrays using textured ZnO seeds, Nano Lett. 5 (2005) 1231‑1236, https://doi.org/10.1021/nl050788p.
[28] Irene Gonzalez-Valls, Monica Lira-Cantu, Vertically-aligned nanostructures of ZnO for excitonic solar cells: a review, Energy Environ. Sci. 2 (2009) 19‑34, https://doi.org/10.1039/b811536b.
[29] RRUFF, All - RRUFF Database Raman, X-ray, Infrared, and Chemistry, http://rruff.info/all/display=default/, (accessed July 2018).
[30] Ü. Özgür, Ya.I. Alivov, C. Liu, A. Teke, M.A. Reshchikov, S. Doğan, V. Avrutin, S.-J. Cho, H. Morkoç, A comprehensive review of ZnO materials and devices, J. Appl. Phys. 98 (2005) 11, https://doi.org/10.1063/1.1992666.
[31] Aleksandra B. Djurišić, Yu Hang Leung, Optical properties of ZnO nanostructures, Small 2 (2006) 944‑961, https://doi.org/10.1002/smll.200600134.
[32] A.B. Djurišić, A.M.C. Ng, X.Y. Chen, ZnO nanostructures for optoelectronics: material properties and device applications, Prog. Quantum Electron. 34 (2010) 191‑259, https://doi.org/10.1016/j.pquantelec.2010.04.001.
[33] Y.S. Wang, P.John Thomas, P. O’ Brien, Optical properties of ZnO nanocrystals doped with Cd, Mg, Mn, and Fe ions, J. Phys. Chem. B 110 (2006) 21412‑21415, https://doi.org/10.1021/jp0654415.
[34] Enamul H. Khan, Marc H. Weber, Matthew D. McCluskey, Formation of isolated Zn vacancies in ZnO single crystals by absorption of ultraviolet radiation: a combined study using positron annihilation, photoluminescence, and mass spectroscopy, Phys. Rev. Lett. 111 (2013) 017401, , https://doi.org/10.1103/PhysRevLett.111.
017401.

Figures

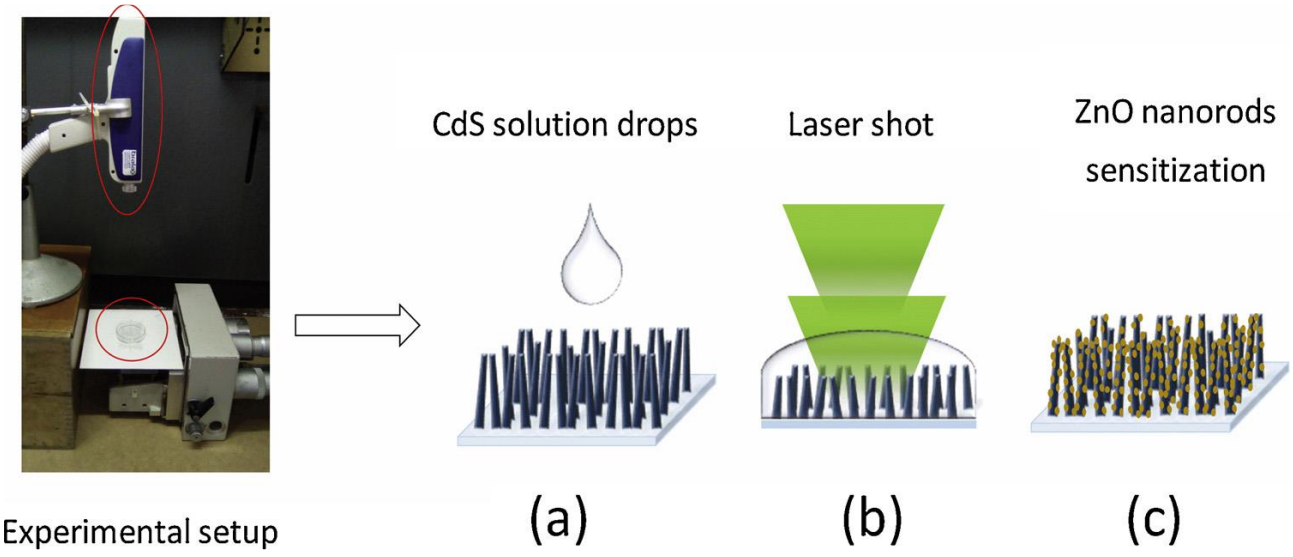

Fig. 1. Laser induced growth to obtain the ZnO/CdS core/shell structures. Red circles in the experimental setup frame the laser (bigger circle) and the sample holder (smaller circle). The fluence and number of laser shots are the main studied parameters (For interpretation of the references to colour in this figure legend, the reader is referred to the web version of this article).

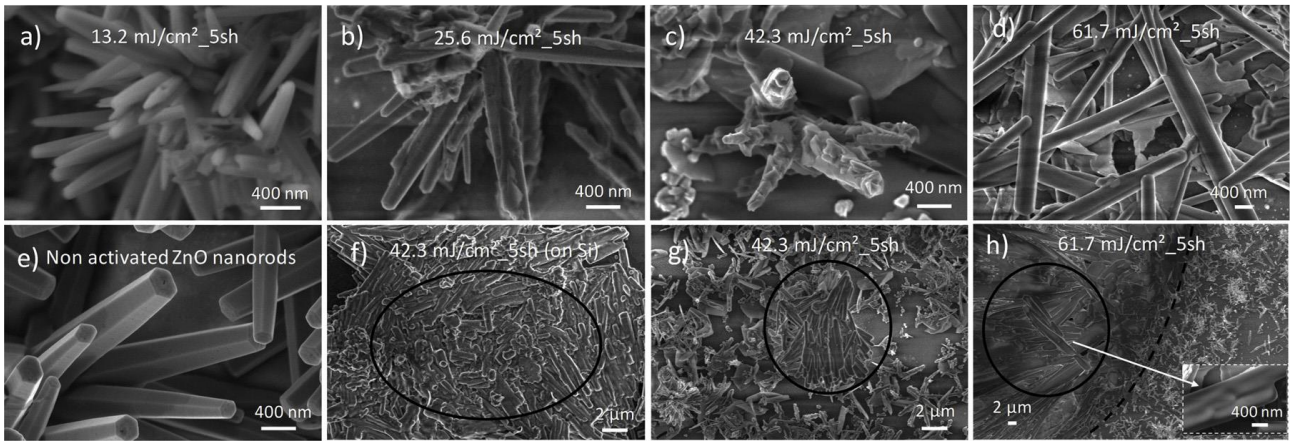

Fig. 2. SEM images from the heterostructures obtained on glass by pulsed laser irradiation: a) ZnO/CdS (13.2 mJ/cm2, 5 shots), b) ZnO/CdS (25.6 mJ/cm2, 5 shots), c) ZnO/CdS (42.3 mJ/cm2, 5 shots), d) ZnO/CdS (61.7 mJ/cm2, 5 shots) and e) as grown ZnO nanorods (no seeded, stirred growth). Images f), g) and h) show the formation of rods-like structures after laser irradiation for three samples: Si/CdS (42.3 mJ/cm2, 5 shots), ZnO/CdS (42.3 mJ/cm2, 5 shots) and ZnO/CdS (61.7 mJ/cm2, 5 shots), respectively. Black circles enclose those structures and dashed line in h) divides the zone where the laser impacted (left part) from the external zone.

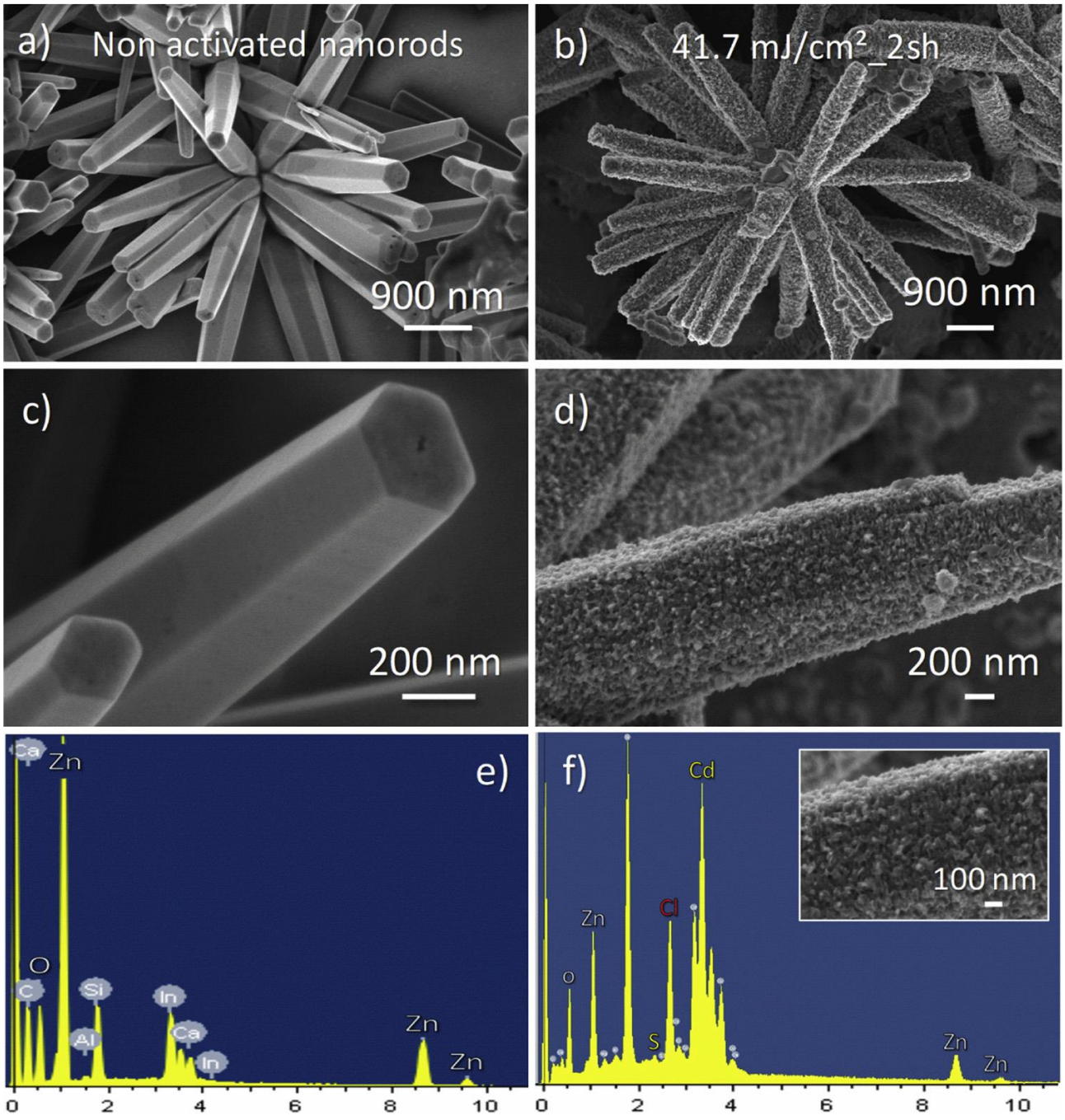

Fig. 3. SEM images of: a) and c) ITO/ZnO nanorods before laser interaction (stirred growth), b) and d) ITO/ZnO/CdS sample where it was obtained the expected core/shell structure (41.7 mJ/cm2, 2 shots), e) and f) corresponding EDS spectra.

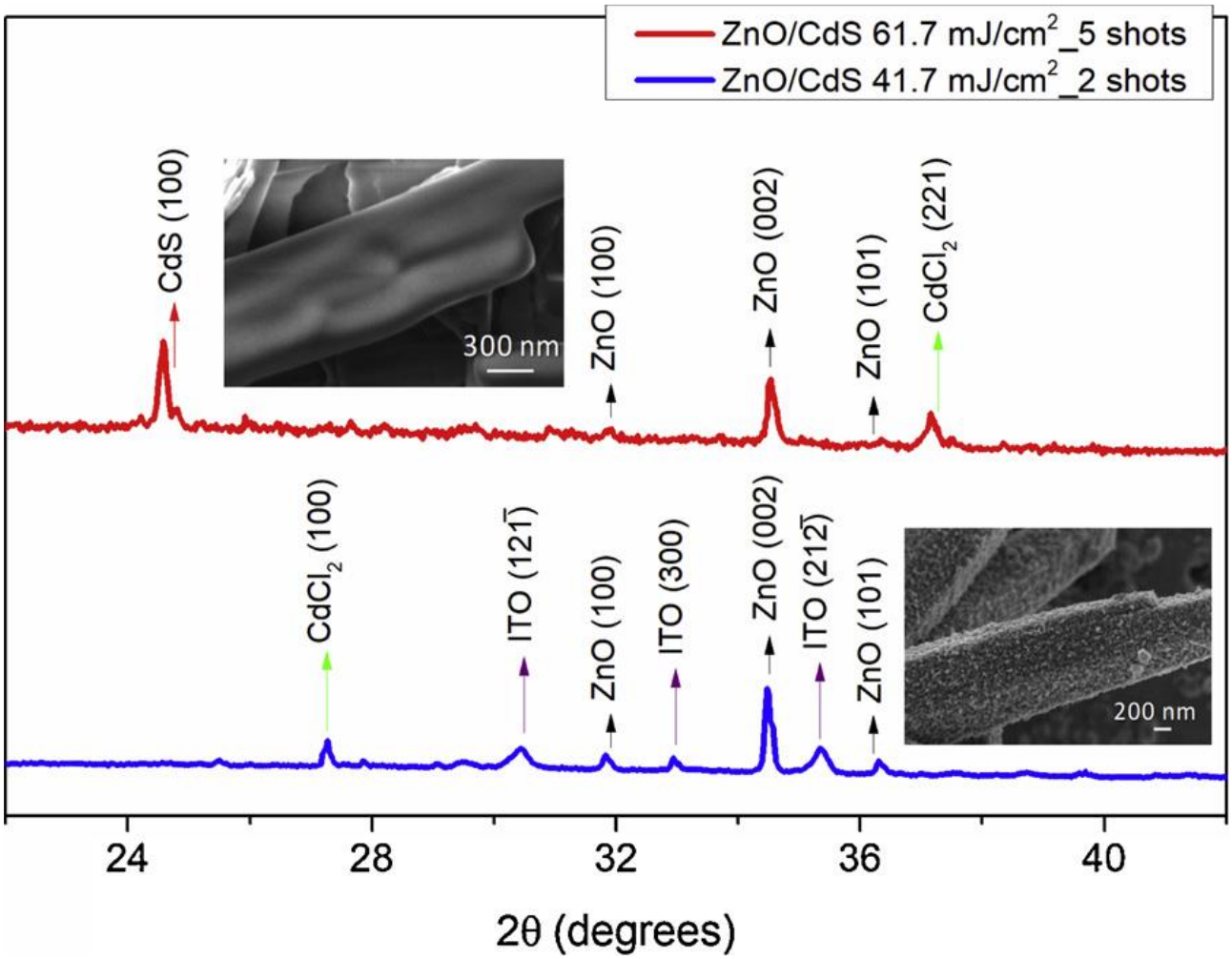

Fig. 4. XRD patterns for ZnO/CdS heterostructures irradiated with laser fluences of 41.7 mJ/cm2 (2 shots) and 61.7 mJ/cm2 (5 shots) respectively. SEM images have been added in each case to better understanding and visualization of the results.

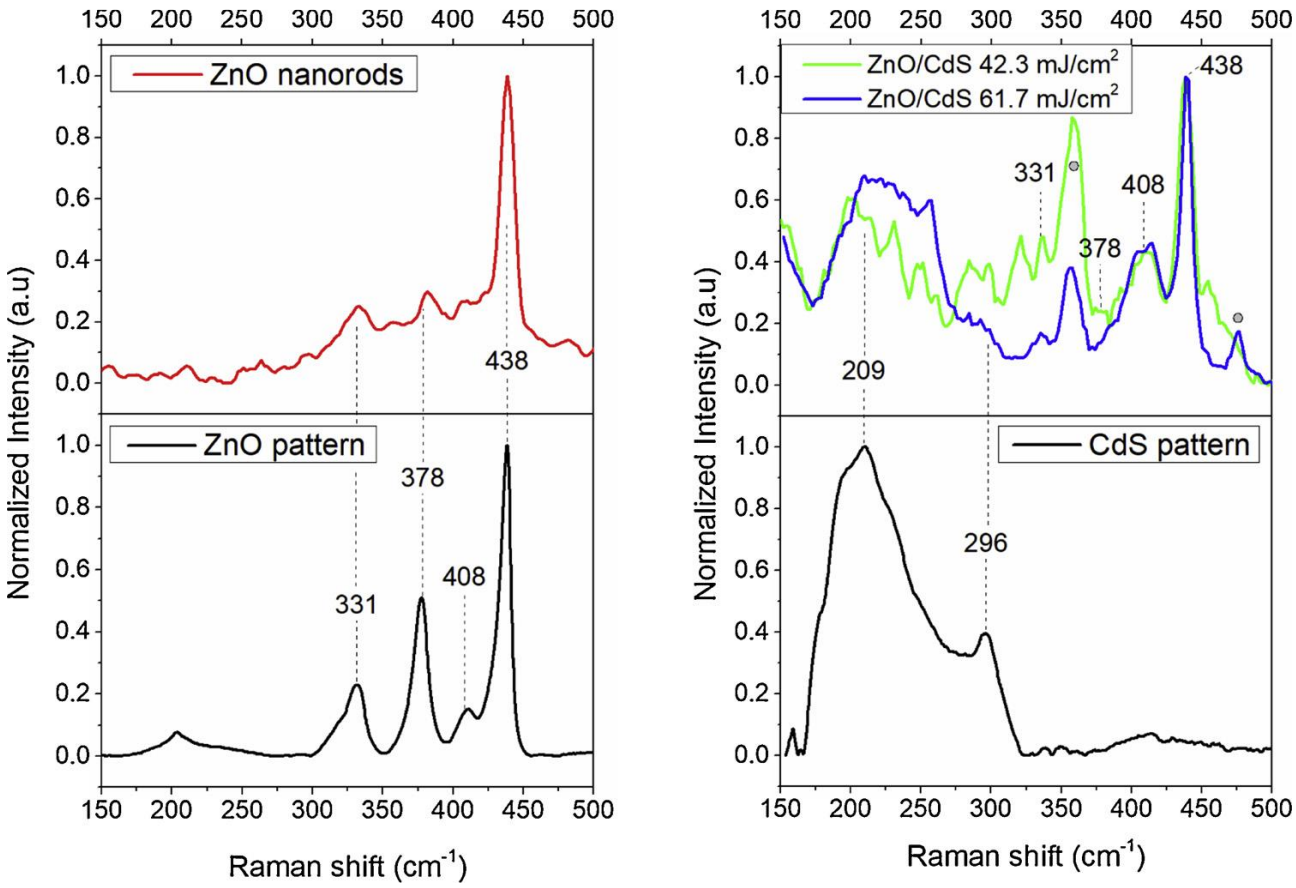

Fig. 5. Raman spectra corresponding to: (left) ZnO nanorods and ZnO standard pattern [29], (right) ZnO/CdS structures (42.3 mJ/cm2 and 61.7 mJ/cm2, 5 shots) and CdS standard pattern [29]. Peaks marked with circles are attributed to defects or residues.

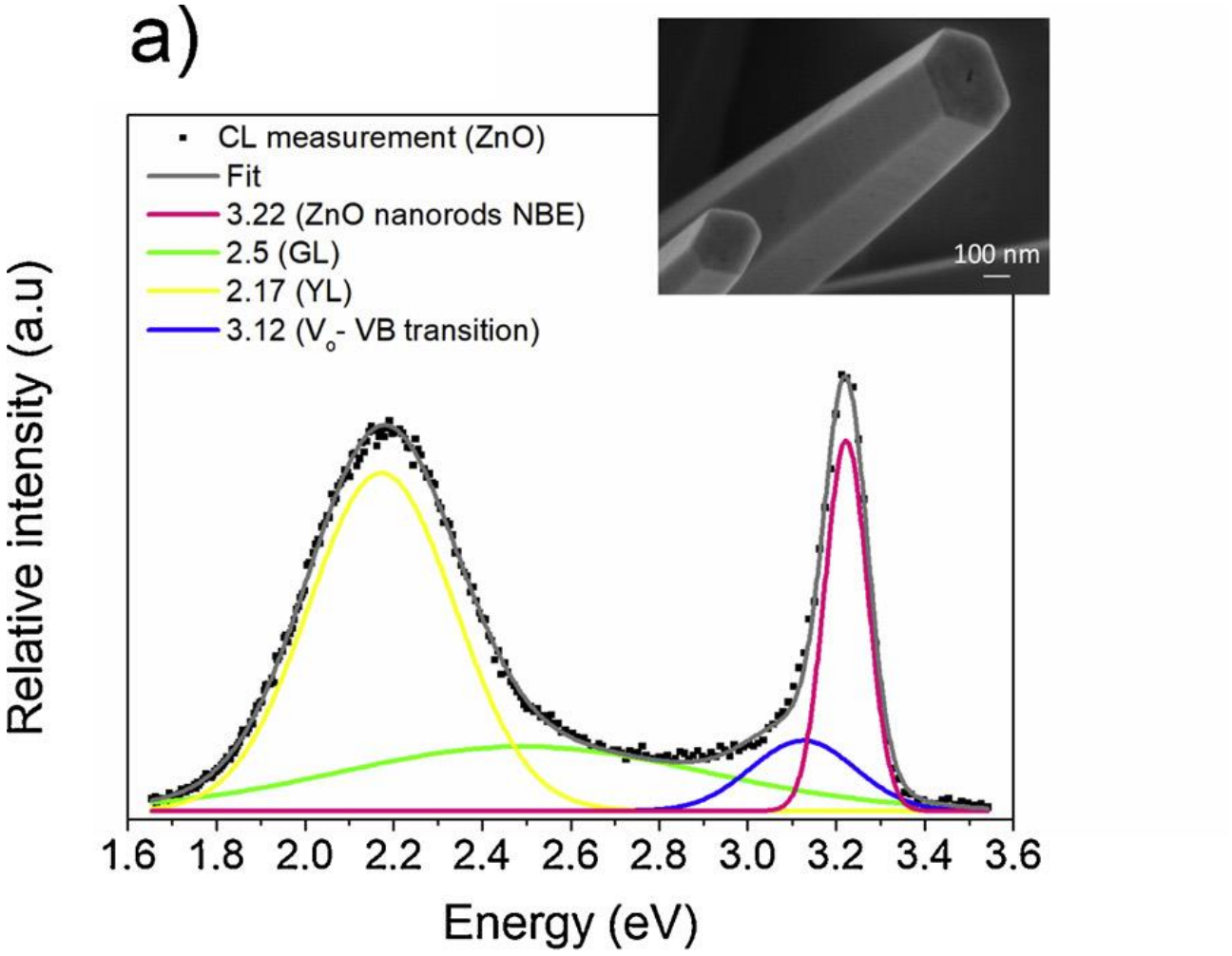
a)
CL measurement (ZnO)
Fit
3.22 (ZnO nanorods NBE)
2.5 (GL)
2.17 (YL)
3.12 (V$_o$- VB transition)
100 nm
Relative intensity (a.u)
1.6 1.8 2.0 2.2 2.4 2.6 2.8 3.0 3.2 3.4 3.6
Energy (eV)

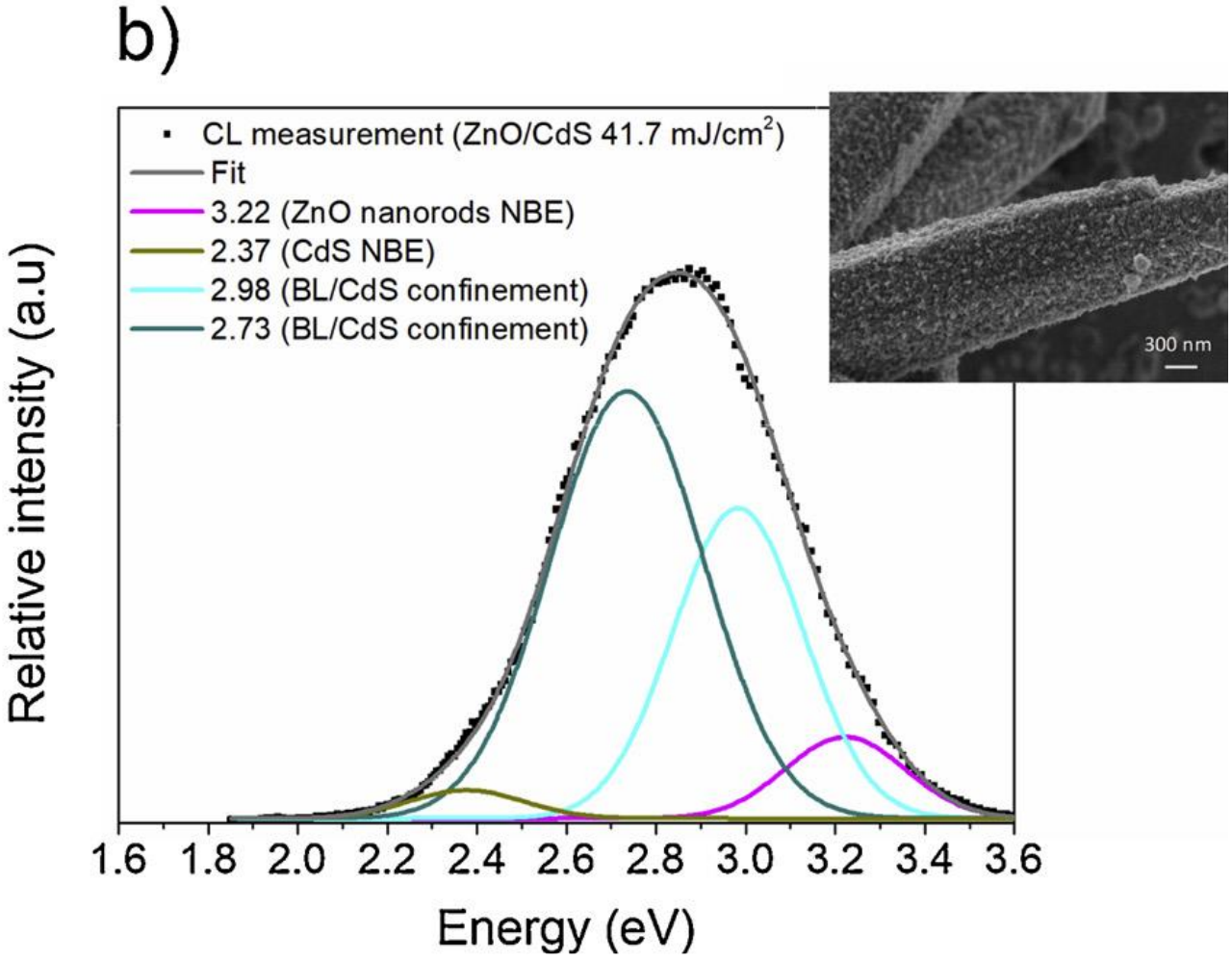
b)
CL measurement (ZnO/CdS 41.7 mJ/cm^2)
Fit
3.22 (ZnO nanorods NBE)
2.37 (CdS NBE)
2.98 (BL/CdS confinement)
2.73 (BL/CdS confinement)
300 nm
Relative intensity (a.u)
1.6 1.8 2.0 2.2 2.4 2.6 2.8 3.0 3.2 3.4 3.6
Energy (eV)

Fig. 6. CL spectra is shown for ZnO nanorods before (a) and after (b) being covered with CdS by laser induced growth (41.7 mJ/cm2, 2 shots). The Gaussian deconvolution helps to understand the contribution of several effects to the original pattern.